Spatial distribution of extreme precipitation in the Tibetan Plateau and effects of external forcing factors based on Generalized Pareto Distribution

Jiajia Gao, Pengfei Ma, Jun Du and Xiaoqing Huang

ABSTRACT

The daily precipitation data of the years 1955–2017 from May to September were retrieved; then a Generalized Pareto Distribution (GPD) and maximum likelihood methods were adopted to understand trends and calculate the reappearance period of heavy precipitation in the Tibetan Plateau (TP). The daily precipitation values at 22 stations in the TP were found to conform to the model, and theoretical and measured frequencies were consistent. According to the spatial distribution of the maximum precipitation value, the extreme values of Shigatse and Lhasa showed large fluctuations, and the probability of record-breaking precipitation events was low. In the western part of Nagqu, the probability of extreme precipitation was relatively low, and that of record-breaking precipitation was relatively high. The peak values of extreme precipitation in the flood season in the TP generally exhibited a decreasing trend from southeast to northwest, and the extreme value of the flood season that reappeared in the southeast region was approximately twice that of the northwest region. The maximum rainfall in most areas will exceed 20 mm in the next 5–10 years, and the maximum rainfall in Shigatse will reach 52.7 mm. After 15 years of recurrence in various regions, the peak rainfall in the flood season has become low. Most of the regions in the model have different responses to ENSO and Indian Ocean monsoon indices with external forcing factors.

Key words | external forcing, GPD, strong precipitation, Tibetan Plateau

Jiajia Gao (corresponding author)
Jun Du
Key Laboratory of Tibet Autonomous Region,
Lhasa 850000,
China;
Lhasa branch, Chengdu Plateau Meteorological Institute of China Meteorological Administration,
Lhasa 850000,
China
and
Institute of Atmospheric And Environmental Sciences, Tibetan Plateau,
Lhasa 850000,
China
E-mail: *1015102649@qq.com*

Pengfei Ma
Xiaoqing Huang
Tibet Climatic Center,
Lhasa 850000,
China

HIGHLIGHTS

- The Generalized Pareto Distribution method was first used in the TP.
- The fitting results agree with the observation results.
- The probability of breaking records was higher due to the lower probability of extreme precipitation.
- The recurrence period of extreme precipitation gradually decreases from southeast to northwest in the TP.
- ENSO and SST index for the Indian Ocean has a great influence on the extreme precipitation in the TP.

INTRODUCTION

Regional floods, droughts, high temperatures, snow and ice storms and other extreme events have occurred frequently due to global climate warming, especially since the 1980s (IPCC 2001; Liu *et al.* 2007). Extreme precipitation is one of the most concerning and influential natural threats, and it is the focus of climate prediction research (Ding *et al.* 2011). To study extreme precipitation and to improve prediction accuracy are crucial ways for establishing a modern

doi: 10.2166/ws.2020.365

public safety system and disaster prevention and mitigation strategy.

Many scholars have used extreme value theory to study extreme climate. Leadbetter *et al.* (1983) used the extreme value distribution of statistical probability to calculate climatic extreme values that occur once every 10–100 years and obtained the correlation between climatic extreme values and average climatic statistical parameters. Groisman *et al.* (1999) suggested that variation in precipitation variance and average value affect the extreme precipitation frequency, and the precipitation showed a nonlinear increasing trend. Byung-Jin *et al.* (2015) used the extreme value theory to study the correlation between daily precipitation and extreme climate. However, the extreme value theory based model dealing with a time series at a point in space is insufficient to reveal spatial distribution of regional extreme climate. Pickands (1975) first proposed the Generalized Pareto Distribution (GPD) and applied it into hydrometeorological research. In recent years, the research on the theory and application of GPD statistics has made rapid progress. The GPD method uses the data above the threshold as the sample data to model, and the extreme data is described accurately. The GPD model has been well validated in eastern China and Chongqing, China (Cheng *et al.* 2008; Jiang *et al.* 2009). Zhao & Zhai (2015) improved the GPD model and got a better extremum distribution parameter, and the result was better than that of the linear moment method.

Linear correlation between the atmospheric circulation and precipitation was proposed in many studies. The circulation anomaly not only increases land surface temperature, but also changes global precipitation (Wallace *et al.* 1996). Some studies have indicated that when strong El Niño-Southern Oscillation (ENSO) events occur, through remote correlation, persistent droughts and floods will occur in some parts of the world, and extremely heavy precipitation events will occur in non-tropical regions (Zhang *et al.* 2017; Hu *et al.* 2018; Liu *et al.* 2018; Yang *et al.* 2018). In addition, ENSO impacts the South Asian summer monsoon by modulating the vertical coupling of the different levels of circulation over South Asia (Liu *et al.* 2015; Jing *et al.* 2017).

The Tibetan Plateau (TP) is located in a geographical location that is in the main sensitive to global climate change. The occurrence of extreme events is an important response to regional climate change. Few studies have forecasted precipitation in the flood season by using the GPD method; therefore, the distributed parameter model of GDP, mainly to exceed the threshold data as sample data modeling, starting from extreme climate distribution, revealed the development rule of extreme precipitation to explore its probability. GPD is expected to provide an improved analysis of extreme events and provide a scientific basis for disaster prevention and mitigation in this article.

MATERIALS AND METHODS

Study area

The TP has average altitude of 4,000 m and a semi-arid monsoon climate in the plateau temperate zone (Figure 1). Due to the high altitude, the temperature of the TP is much lower than in other the regions of the same latitude. The average temperatures during spring, summer, autumn, winter are −11.2 °C to −2.5 °C, 7.1 °C to 18.5 °C, −2.4 °C to 12.9 °C, and −13.4 °C to 5.0 °C, respectively. The annual precipitation is 66.3–894.5 mm. The annual precipitation in most regions of Nyingchi is >600 mm, while that in Ali is <200 mm. With the alternating influence of the west wind in winter and the southwest monsoon in summer, the dry season and rainy season are clear. The rainy season is from May to September, and it generally accounts for approximately 90% of the annual precipitation. Furthermore, the precipitation is extremely uneven in different regions, gradually decreasing from Nyingchi to Ali.

The topography of the TP is relatively complex, and it is mainly composed of high mountains and valleys. It has various vegetation types. The southeast of the TP is at a low altitude and mainly includes broadleaf forest, coniferous forest, and shrubs. The north and northwest regions have meadows, steppe, and desert.

Data

The study data were taken from the Information Network Center of Tibet Meteorological Bureau. All data were tested for temporal and spatial consistency.

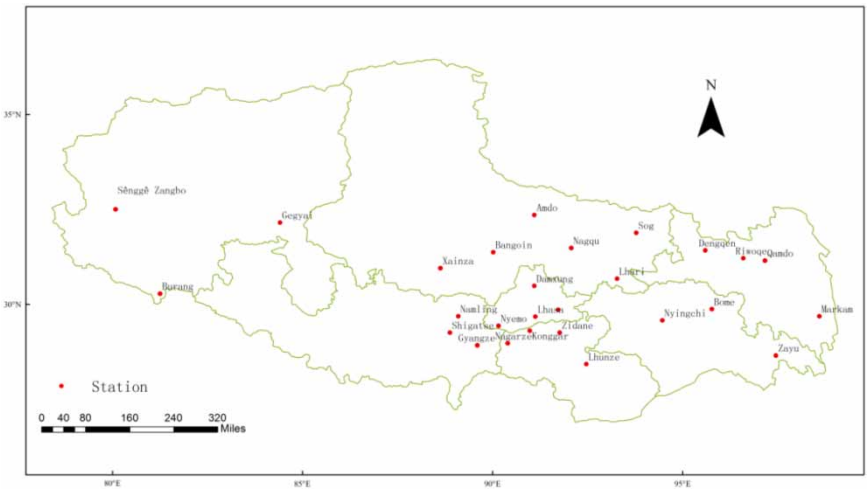

Figure 1 | Location of the study area.

The study data consisted of daily precipitation data of 22 stations in the TP over the past 50 years (1955–2017) from May to September. Observation data of some weather stations were from in 1955, 1961, and 1978 (Table 1). The circulation index and sea surface temperature (SST) index were obtained from NOAA.

Density and distribution function

The GPD can directly use the original data over the years to set the threshold value artificially. After setting the threshold value, the maximum or minimum value exceeding the threshold value every year was extracted based on the criterion known as 'peaks over threshold' (Beirlant *et al.* 1996):

$$\left\{\left(\mu,\ \frac{1}{n}\sum_{i=1}^{n_\mu}(x_i-\mu)\right),\quad \mu < x_{\max}\right\} \tag{1}$$

The distribution function of the GPD is obtained as follows:

$$f(x) = 1 - \left[1 - k\left(\frac{x-\xi}{a}\right)\right]^{1/k} \qquad k \neq 0, \xi \leq x \leq \frac{a}{k} \tag{2}$$

The density function of the GPD is obtained as follows:

$$f(x) = \frac{1}{a}\left[1 - k\left[\frac{x-\xi}{a}\right]\right]^{1/k-1} \tag{3}$$

Table 1 | Basic information of each stations in the TP

Station	Longitude	Latitude	Station	Longitude	Latitude
Amdo	91.1	32.35	Markam	98.6	29.68
Bangoin	90.02	31.37	Nagarze	90.4	28.96
Burang	81.25	30.28	Nagqu	92.07	31.48
Dengqen	95.6	31.42	Namling	89.1	29.68
Gegyai	84.41	32.15	Nyingchi	94.47	29.57
Gyangze	89.6	28.91	Qamdo	97.17	31.15
Konggar	90.98	29.30	Riwoqe	96.6	31.21
Lhari	93.28	30.66	Sênggê Zangbo	80.08	32.5
Lhasa	91.13	29.67	Shigatse	88.88	29.25
Lhunze	92.47	28.42	Zayu	97.46	28.65
Maizhokunggar	91.73	29.85	Zidane	91.76	29.25

The GPD includes three main parameters, namely location ξ, which is similar to the mathematical expectation of general distribution, scale parameter a, and shape parameter k. When $k < 0$, $\xi < x < \infty$; when $k > 0$, GPD is an exponential distribution; and $k = 1$, GPD is uniformly distributed on the interval $[\xi, \xi + a]$.

Maximum likelihood parameter estimation

The maximum likelihood is calculated as follows:

$$L = \left(\frac{1}{a}\right)^N \prod_{i=1}^{N} \left[1 - \frac{k}{a}(x_i - \xi)\right]^{1/k-1} \quad (4)$$

The logarithmic likelihood is calculated as follows:

$$\log L = -N \log(a) + \left(\frac{1}{k} - 1\right) \sum_{i=1}^{N} \log(y_i) \quad (5)$$

This is an increasing function of ζ, and the estimated value of ζ is the minimum value X_1 of the observation series. According to the Newton iteration method, other parameters can be obtained by combining the following three equations:

$$\frac{\partial \log L}{\partial a} = \frac{1}{a}(1/k - 1) \sum_{i=1}^{N} y_i^{-1} - \frac{N}{aK} = 0 \quad (6)$$

$$\frac{\partial \log L}{\partial k} = \frac{N}{k}\left(\frac{1}{k} - 1\right) - \frac{1}{k^2} \sum_{i=1}^{N} \log(y_i) - \frac{1}{k}\left(\frac{1}{k} - 1\right) \sum_{i=1}^{N} y_i^{-1} = 0 \quad (7)$$

$$y_i = 1 - \frac{k}{a}(x_i - \xi) \quad (8)$$

Recurrence period

Precipitation fraction at time T in a certain recurrence period is as follows:

$$\hat{x} = \hat{\xi} + \frac{\hat{a}}{\hat{k}}(1 - T^{-\hat{k}}) \quad (9)$$

Data processing and statistics

MATLAB® was used for statistical analysis of the data. Data that did not follow a normal distribution were transformed. The correlation coefficient was tested by using the t test, and $p < 0.05$ indicated a significant result.

RESULTS AND DISCUSSION

Selection of threshold value

Threshold is the premise of parameter estimation. If the threshold is high, the estimated parameter variance will be large; if it is low, the function condition cannot be satisfied. The estimator will become biased, leading to function divergence. We adopted the method of dynamic threshold estimation; that is, within a certain threshold range, the shape and scale parameters of the equation larger than the threshold should remain unchanged.

The observation records of most stations in the TP began in the mid and late 1950s. To meet the equation requirements, we selected 22 stations with complete observation records and data of 30–50 years. First, by arranging the observed data in a descending order, the threshold value between 90th and 99th percentiles can be calculated. Then, according to the Equations (6)–(8), the corresponding shape and scale parameters can be calculated.

The results of the Lhasa station (Table 2) showed that the shape parameter with the observed value between the

Table 2 | Test of estimated parameters under different thresholds for the GPD model

Percentile	ξ	a	k	K-S
0.9	9.4	6.95	−0.047	0.061
0.91	10.2	6.17	−0.034	0.064
0.92	11	6.64	−0.027	0.078
0.93	11.9	6.52	−0.019	0.083
0.94	12.9	6.57	−0.024	0.082
0.95	14.1	6.52	−0.022	0.086
0.96	15.5	6.54	−0.028	0.078
0.97	17.3	6.55	−0.048	0.085
0.98	19.9	6.53	0.029	0.087
0.99	23.7	9.05	−0.269	0.08

93rd and 98th percentiles was stable at approximately 6.5. However, for the 98th percentile (Kolmogorov–Smirnov, K-S), the value is the highest at approximately 0.087. Therefore, we choose the observed value of the 98th percentile as the threshold value.

Model fitting effect test

To test whether the model conformed to the known theoretical distribution function, the Kolmogorov method was used in this study. Most sites with $p > 0.05$ confirmed the null hypothesis (Figure 2(a)). The daily strong precipitation during the flood season of the TP basically conforms to the model. Although differences were observed between stations, the GPD fitting curve showed that the theoretical frequency was consistent with the measured frequency.

We selected Lhasa, Sênggê Zangbo (Ali), and Kongga stations as representative stations, with their records starting from 1955, 1961, and 1978, respectively (Figure 2(b)–2(d)). The results showed that the data length does not affect the statistical inference of precipitation extremum, and the longer the data period, the better the fitting results.

We calculated the errors corresponding to different cumulative frequencies (Table 3). When the cumulative frequency was low, almost no error occurred. With an increase in the cumulative frequency, the error gradually increased. In particular, when the cumulative frequency of Kongga station was 0.9, the error reached 1.1, indicating that the length of the research period does not affect the simulation effect, and the random error of the equation itself might be one of the reasons for the large error.

Spatial distribution of precipitation extremum

The scale parameter mainly describes the variability of extremum distribution. The range of extreme value fluctuation increases with an increase in scale parameter. The average scale parameter of precipitation extremum in the TP was 6.07 ± 1.47. Table 4 shows that the scale parameter gradually decreased from north to south, and the maximum value was observed near Shigatse and Lhasa, indicating

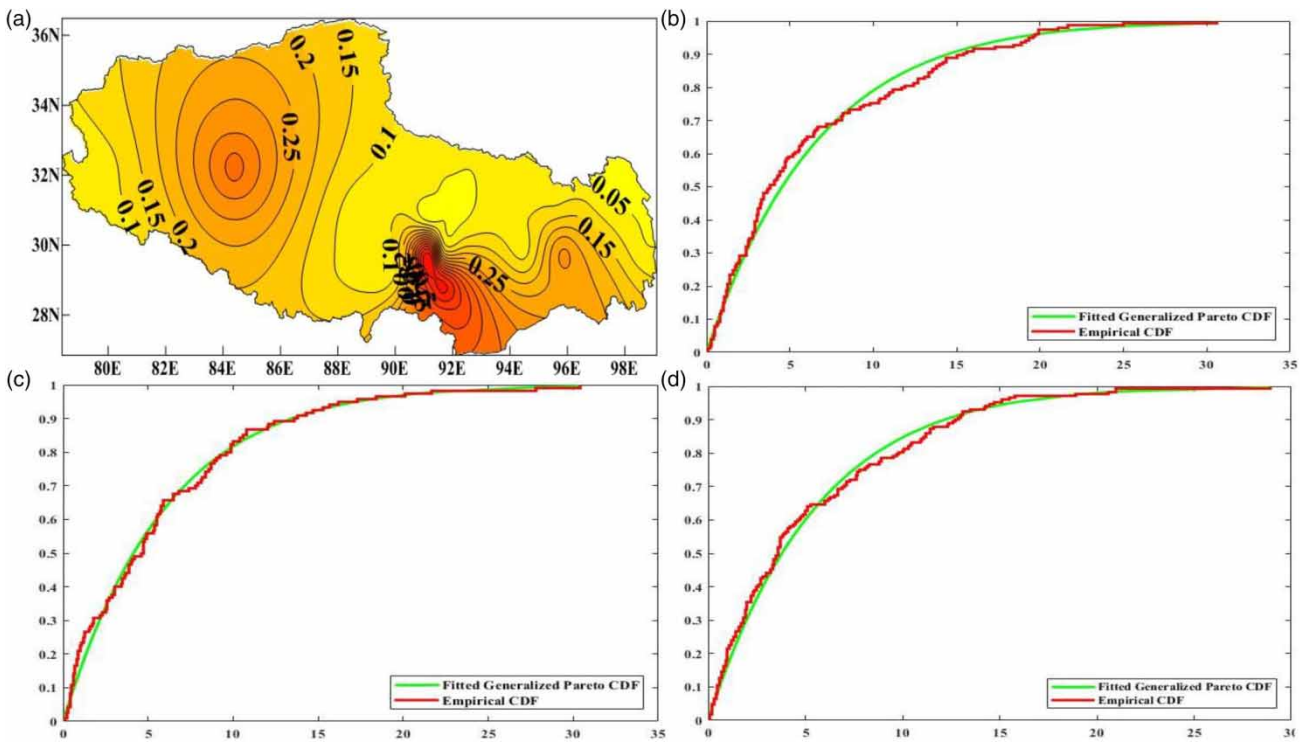

Figure 2 | K-S test for comparing measured and cumulative frequency distribution curves of TP. (a): All stations of TP passed the K-S test distribution. Measured frequency and cumulative frequency distribution curves of (b) Lhasa. Measured frequency and cumulative frequency distribution curve of Kongga Station (c) and that of Sênggê Zangbo Station (d).

Table 3 | Standard errors corresponding to different cumulative frequencies

	Standard error of observed and fitted values		
Cumulative frequency	**Lhasa**	**Sênggê Zangbo**	**Kongga**
0.1	0	0	0
0.2	0.176	0	0
0.3	0	0	0.247
0.4	0.021	0.141	0.141
0.5	0.014	0	0
0.6	0	0	0
0.7	0.282	0.141	0
0.8	0.070	0.636	0.608
0.9	0.507	0.424	1.060

Table 4 | Scale and shape parameters of each region

Station	a	k	Station	a	k
Amdo	0.0334	4.67	Markam	−0.1	7.35
Bangoin	0.11	3.8	Nagarze	−0.58	11.76
Burang	−0.057	5.97	Nagqu	−0.049	4.95
Dengqen	−0.075	5.98	Namling	−0.027	5.98
Gegyai	−0.058	5.87	Nyingchi	0.048	5.26
Gyangze	−0.007	5.44	Qamdo	−0.07	6.73
Konggar	−0.023	5.39	Riwoqe	−0.005	5.25
Lhari	−0.04	5.79	Sênggê Zangbo	−0.047	5.57
Lhasa	−0.056	6.66	Shigatse	−0.15	6.99
Lhunze	−0.027	5.33	Zayu	0.17	5.69
Maizhokunggar	−0.14	6.38	Zidane	−0.14	5.84

that the extreme value in this region fluctuates greatly. From the climatic background perspective, Lhasa and Shigatse are located in the plateau monsoon region, which is affected by the Indo-Myanmar trough and the westerlies, and the seasonal precipitation is relatively high (Yang *et al.* 2014; Ma *et al.* 2016). Furthermore, it is related to the urbanization of the two regions. Because the urban characteristics change the local overhead circulation, different urbanization development stages will lead to different spatial precipitation structures, especially during the rapid urbanization period, the precipitation frequency will increase (Jiang & Li 2014; Zheng *et al.* 2014; Zhang *et al.* 2015). Moreover, IPCC has used humanistic factors to diagnose changes in the spatial pattern of regional precipitation. The secondary value area is located near Nyingchi. Because this region is located in the South Tibetan Valley, its altitude is lower than that of Lhasa; the rainfall is related to the topography. The Indian Ocean monsoon is influenced by mountains on the southern edge of the TP during its northward advance. The air flows northward along the low-lying Yarlung Zangbo River and its tributaries. During the transmission, the great bend of the Yarlung Zangbo River is sharply uplifted, generating abundant precipitation (Liu *et al.* 2003). Therefore, the extreme precipitation value fluctuates greatly, and it is also a flood-prone region.

The area with the minimum scale parameter was the west of Nagqu. This region is located in the hinterland of the plateau. Precipitation is mainly affected by the cold air from the north. The Tianshan Mountains block the cold air from the south. Therefore, the average daily precipitation intensity in this region is only 2.8 mm, and the number of precipitation days is low, with small fluctuations in the extreme value. This is consistent with the research results of Wan (2010). Most of the arid areas in China are located in non-monsoon areas, with a small range of extreme precipitation values and a low possibility of breaking records.

As the second important parameter of the model, the shape parameter, represents the different tail distribution characteristics of the model. Table 4 shows that the positive area of shape parameters mainly consists of Bangor, Amdo, and other areas, where the possibility of record-breaking precipitation events is higher than in other areas. The negative values of shape parameters were mainly in Shigatse, Lhasa, and other areas along the river, followed by stations in Qamdo, where the probability of precipitation breaking records is relatively low. According to the distribution of corresponding scale parameters, the extreme value variation rate of precipitation along the river and in Nyingchi and other areas is high, and the dispersion degree is larger than the mean value; thus, the probability of breaking the record is low. This is consistent with the synoptic principle that the larger the wavelength, the smaller the frequency. The number of precipitation days in the west of Nagqu is low, and the precipitation variation rate was low. Once precipitation occurs, the extreme state is likely to be a record-breaking behavior. Thus, the more frequent the summer precipitation, the lower the possibility of the extreme value to

break the record. In arid areas, the climatic probability of precipitation is usually low, so the probability of breaking records is high.

Estimation of recurrence period

The TP flood season precipitation extreme value return level generally presents the southeast northwest high low, from southeast to northwest gradually decreasing, and southeast to reproduce the extreme flood season is about two times that of in northwest China, but also reflects Nyingchi as the most serious secondary disasters caused by heavy rainfall, in agreement with the observation (Table 5). In terms of the extreme value levels of the 5- and 10-year reoccurring flood seasons, the extreme value of rainfall in regions other than Sênggê Zangbo exceeded 20 mm, and the extreme precipitation value of Shigatse reached 52.7 mm. Furthermore, the extreme distribution values of Lhasa and Nyingchi were high. Li & Li (2015) observed that when the temperature increased by 2 °C, the percentage of heavy precipitation anomaly on the TP increased by 44.5–59.5% on average, with a large value near Shannan City. With a recurrence period of 15 years, the increase in precipitation extremum in the flood season was low; growth was slowest for Nyingchi, with a rate of 1.6 mm/5a. The maximum rainfall in Shigatse increased at the fastest rate of approximately 3.6 mm/5a. Studies have shown that extreme precipitation frequency in Tibet is generally >4.3 times per year, and the intensity is >20 mm/d. Nyingchi is a high-value region of extreme rainfall, and the frequency of extreme precipitation along the Yajiang River is increasing (Song *et al.* 2013; Yuan *et al.* 2014). One of the most important purposes for establishing an extreme value model is to predict the recurrence period or recurrence level of extreme events. However, 'recurrence period' does not refer to the 'cycle' that will definitely appear after T years but the 'statistical cycle' in the probability sense.

Table 5 | Maximum daily precipitation (mm) during summer in the main areas of the TP for various recurrence periods

	Recurrence period (year)					
Station	**5**	**10**	**15**	**20**	**25**	**30**
Lhasa	31.1	36.3	39.4	41.6	43.4	44.9
Sênggê Zangbo	15.0	19.2	21.8	23.6	25.1	26.2
Naqu	24.7	28.5	30.7	32.4	33.7	34.7
Zedane	29.4	34.8	38.1	40.6	42.6	44.3
Nyingchi	31.4	34.8	36.7	38.0	39.0	39.8
Shigaze	34.4	40.9	45.1	48.1	50.6	52.7
Qamdo	29.8	35.1	38.4	40.7	42.6	44.1

Influence of external forcing factors on extreme precipitation

To understand the influence of external forcing factors on the shape and scale parameters, linear trend terms were added to the model parameters. The external forcing factors we selected were ENSO and the Indian Monsoon Index (ID), which are related to precipitation over the TP. ENSO and the Indian Ocean SST index forcing terms were added to the scale and shape parameters, respectively:

$$\text{GPD1:}\begin{cases}\xi = const\\ \log a_r = a_{0r} + a_{1r}ENSO(t)\\ \log k_r = k_{0r} + k_{1r}ENSO(t)\end{cases}$$

$$\text{GPD2:}\begin{cases}\xi = const\\ \log a_r = a_{0r} + a_{1r}ID(t)\\ \log k_r = k_{0r} + k_{1r}ID(t)\end{cases}$$

where t represents time, a_0 and k_0 represent the linear growth trends of the scale and shape parameters, respectively, and a_1t and k_1t represent the covariables of linear increment. To ensure that the data are positive, scale and shape parameters were transformed into their logarithmic forms. In GPD1, the shape parameter was fixed, and the scale parameter was added with an external forcing factor. In GPD2, the scale parameter was fixed, and the shape parameter was added with an external forcing factor.

To assess whether these models improved on the original model, a test judgment must be made. The method and procedure of judgment are described below. Suppose the GPD model without a covariable factor is M_0, whereas the GPD model with covariable factor is M_1; θ_0 and θ_1 are the parameter vectors, and $M_0 \in M_1$:

$$D = 2[l_1(M_1) - l(M_0)]$$

where $l_1(M_1)$and $l(M_0)$ represent the maximum value of the

logarithmic likelihood functions of M_1 and M_0 respectively. D obeys the chi-square distribution. If at the significance level of 5%, $D > C_{1\text{-a}}$, and $C_{1\text{-a}}$ is the distribution quantile of ξ_k^2, then the null hypothesis, namely M_1, is better able to describe the data.

The results showed that the scale and shape parameters changed when the two external forcing factors were added (Table 6). When ENSO was added, the change amplitude of the shape parameter was higher than that of the scale parameter. The range of the scale parameter was −0.2 to 0.33. The scale parameters of Burang, Gyangze, Lhari, Lhunze, Maizhokunggar, Markam, Shigatse, and Zidane exhibited an increasing trend. However, the scale parameter did not change in Sênggê Zangbo. Thus, ENSO has no effect on the scale parameter in the Sênggê Zangbo area. After ENSO was added to the shape parameter, the value increased. This indicated that the probability of breaking the extreme precipitation value in most areas also increased. After adding the ID influence factor, the scale parameter exhibited a negative value in most areas, and the range was −0.16 to 0.087. The shape parameters in most areas exhibited limited numerical change after the ID factor was added.

Table 6 | Influence of external forcing on various parameters

	GPD1		GPD2	
Station	**a**	**k**	**a**	**k**
Amdo	0.0334	4.67	0.0335	5.18
Bangoin	0.11	3.8	0.17	4.6
Burang	−0.057	5.97	0.01	4.37
Dengqen	−0.075	5.98	−0.062	4.05
Gegyai	−0.058	5.87	−0.023	4.88
Gyangze	−0.007	5.44	0	4.58
Konggar	−0.023	5.39	−0.11	4.99
Lhari	−0.04	5.79	−0.035	4.71
Lhasa	−0.056	6.66	−0.029	5.62
Lhunze	−0.027	5.33	−0.023	4.4
Maizhokunggar	−0.14	6.38	−0.17	4.61
Markam	−0.1	7.35	−0.03	3.07
Nagarze	−0.58	11.76	−0.58	3.74
Nagqu	−0.049	4.95	−0.045	5.58
Namling	−0.027	5.98	−0.023	4.87
Nyingchi	0.048	5.26	0.077	4.58
Qamdo	−0.07	6.73	−0.01	3.98
Riwoqe	−0.005	5.25	0.03	4.39
Sênggê Zangbo	−0.047	5.57	−0.03	4.42
Shigatse	−0.15	6.99	−0.06	4.32
Zayu	0.17	5.69	0.33	4.96
Zidane	−0.14	5.84	−0.09	4.11

In general, the southeastern region of the TP is strongly affected by ENSO, whereas the southern marginal region is strongly affected by ID. Along the Yarlung Zangbo River to Qamdo, both indexes have a substantial influence, with a gradual decline from southeast to northwest.

The effect of these two forcing factors can be ignored in Ali due to its geographical location. The summer precipitation is only slightly affected by SST, which may be caused by the southward movement of cold air from the north or the small amount of water vapor carried by the westerly belt. Moreover, Nyingchi is located in the eastern section along the Yangtze River, and the external forcing effect of ENSO is smaller than that of the ID factor. Thus, ENSO is not the most important external factor affecting the extreme precipitation value, mainly because the Indian Ocean SST anomaly affects the Indian Ocean monsoon and then affects the distribution of water vapor transport and water vapor flux divergence over the south of the TP through circulation adjustment, finally changing the precipitation pattern. Considering the ENSO and ID factors, their occurrence mechanism and geographical location determine their regional effects on summer extreme precipitation. Different physical mechanisms lead to different climate effects. In the analysis of summer extreme precipitation, the correlation between multiple circulation factors and sea–air coupling is also considered.

CONCLUSION

The probability distribution model of GPD was introduced to simulate the regularity of heavy precipitation during the flood season in the TP. The results showed that the daily heavy precipitation at 22 stations in the TP conformed to the model, and the theoretical frequency was consistent with the measured frequency.

The high-value regions for the scale parameter were located in Lhasa, which indicates that the extreme value

fluctuated greatly. Conversely, the small-value region was located in the west of Nagqu, indicating that the extreme value fluctuated only slightly. The positive region for the shape parameter was mainly located in Nagqu, suggesting that the probability of a record-breaking precipitation event is relatively high. The negative area was mainly in Shigatse, Lhasa, and other areas along the river line, followed by stations in Qamdo, where the probability of extreme precipitation is relatively low.

In the TP, the recurrence of extreme precipitation during the flood season exhibited a gradually diminishing trend from southeast to northwest, from the level of 5 years and 10 years reoccurring flood extreme values including Sênggê Zangbo; other regions with extreme rainfall received >20 mm rainfall. In the TP, the extreme precipitation threshold is 52.7 mm; Lhasa and Nyingchi also have a high extreme value distributions. For a 15-year recurrence, the increase in rainfall extremity in flood season was slow.

Most areas are affected by the external forcing factors of ENSO and ID, which also indicates that these two indexes have a strong influence on extreme precipitation in the TP during summer. In Nyingchi, the forcing effect of ID was greater than that of ENSO.

ACKNOWLEDGEMENTS

This work was supported by the Nature Foundation of Tibet Autonomous Region (XZ-2019ZRG-150). This manuscript was edited by Wallace Academic Editing.

DATA AVAILABILITY STATEMENT

Data cannot be made publicly available; readers should contact the corresponding author for details.

REFERENCES

Beirlant, J., Vynckier, P. & Teugels, J. L. 1996 Tail index estimation, Pareto quantile plots, and regression diagnostics. *Journal of the American Statistical Association* **91** (436), 1659–1667.

Byung-Jin, S., Hyun-Han, K., Dongkyun, K. & Seung Oh, L. 2015 Modeling of daily rainfall sequence and extremes based on a semiparametric Pareto tail approach at multiple locations. *Journal of Hydrology* **529** (3), 1442–1450.

Cheng, B. Y., Ding, Y. G., Zhang, J. L. & Jiang, Z. H. 2008 Application of generalized Pareto distribution to the research of extreme rainfall of Chongqing. *Plateau Meteor* **27** (5), 1004–1009.

Ding, Y. G., Li, J. Y., Jiang, Z. H. & Yu, J. H. 2011 Advances in extremes statistics and their application to climate change study. *Advances in Climate Change Research* **7** (4), 248–252.

Groisman, P., Karl, T. R., Easterling, D. R., Knight, R.W., Jamason, P F., Hennessy, K. J., Suppiah, R., Cher, M. P., Wibig, J., Fortuniak, K., Razuvaev, V. N., Douglas, A., Førland, E. & Zhai, P. M. 1999 Changes in the probability of heavy precipitation: important indicators of climatic change. *Climate Change* **42**, 243–283.

Hu, J., Yan, H. M. & Zhou, J. Q. 2018 The research of antecedent SST signal to east Asia summer monsoon. *Journal of Tropical Meteorology* **34** (03), 401–409.

IPCC Climate Change. 2001 *The Scientific Basis*. Cambridge University Press, Cambridge, United Kingdom and New York, NY, USA, p. 881.

Jiang, Z. H. & Li, Y. 2014 Impact of urbanization in different regions of eastern China on precipitation and its uncertainty. *Journal of Tropical Meteorology* **30** (04), 601–611.

Jiang, Z. H., Ding, Y. G., Zhu, L. F., Zhang, J. L. & Zhu, L. H. 2009 Extreme precipitation experimentation over eastern China based on Generalized Pareto Distribution. *Plateau Meteor* **28** (3), 573–579.

Jing, G., You, H., Valerie, M. D. & Tandong, Y. 2017 ENSO effects on annual variations of summer precipitation stable isotopes in Lhasa, southern Tibetan Plateau. *Journal of Climate.* **31** (3), 1172–1182.

Leadbetter, M. R., Lindgren, G. & Rootzen, H. 1983 Extremes and Related Properties of Random Sequences and Process. New York, Springer-Verlag, 336 pp.

Li, H. M. & Li, L. 2015 Mean and extreme climate change on the Qinghai-Tibetan Plateau with a 2 global warming. *Advances in Climate Change Research* **11** (3), 1673–1719.

Liu, X. H., Qin, D. H. & Shao, X. M. 2003 Variation and abrupt change of precipitation in Nyingchi prefecture of Tibet autonomous region in past 350 years. *Journal of Glaciology and Geocryology* **25** (04), 375–379.

Liu, J. F., Ding, Y. G. & Jiang, Z. H. 2007 The Influence of aggravated global warming on the probability of extreme climatic event. *Plateau Meteor* **26** (4), 837–842.

Liu, B., Wu, G. X. & Ren, R. C. 2015 Influences of ENSO on the vertical coupling of atmospheric circulation during the onset of South Asian summer monsoon. *Climate Dynamic.* **45**, 1859–1875.

Liu, M. H., Ren, L. H., Zhang, W. J. & Ren, P. F. 2018 Influence of super El Niño events on the frequency of spring and summer extreme precipitation over eastern China. *Acta Meteorologica Sinica* **76** (04), 539–553.

Ma, S. Q., Zhou, S. W. & Wang, S. 2016 Diurnal variation characteristics of GPS-retrieved precipitable water vapor over Mid-East Xizang in summer. *Plateau Meteor* **35** (02), 318–328.

Pickhands, J. 1975 Statistical inference using extreme order statistics. *The Annual Statistics* **3**, 119–131.

Song, S. Y., Wang, P. X., Du, J., Yang, Z. G., Jia, L., La, Z. & Zhang, J. 2013 The Climate. *Beijing: China Meteorological Press* **12**, 217–239.

Wallace, J. M., Zhang, Y. & Bajuk, L. 1996 Interpretation of interdecadal trends in northern hemisphere surface air temperature. *Journal of Climate* **9** (2), 249–259.

Wan, S. Q. 2010 Simulation on spatial and temporal distribution of precipitation and temperature extremes in China. *Lanzhou: Lanzhou University* **5**, 100–117.

Yang, Z. G., Jian, J. & Hong, J. C. 2014 Temporal and spatial distribution of extreme precipitation events in Tibet during 1961–2010. *Plateau Meteor* **7** (5), 37–42.

Yang, C. H., Zhang, L., Yuan, G. H., Guo, Q., Sun, N. X. & Du, T. 2018 Characteristics of temperature and precipitation in east Asia and north America. *Plateau Meteor* **37** (03), 662–674.

Yuan, Z., Li, Y., Yang, Z. Y., Yin, J. & Yuan, Y. 2014 Spatio-temporal variation characteristics of extreme precipitation events in Tibet in last 50 years. *Water Resources and Hydropower Engineering* **45** (10), 19–24.

Zhang, S., Huang, G. & Wang, J. 2015 Impact of urban surface characteristics on summer rainfall in the Beijing-Tianjin-Hebei area. *Chinese Journal of Atmospheric Sciences* **39** (05), 911–925.

Zhang, R. H., Min, Q. Y. & Su, J. Z. 2017 Impacts of El Niño on atmospheric circulation over east Asia and rainfall in China: role of the anomalous western North Pacific Anticyclone. *Science China Earth Sciences* **47** (05), 544–553.

Zhao, R. X. & Zhai, Y. M. 2015 Study on Pickands bootstrap moment estimation of generalized Pareto distribution parameters of extreme precipitations. *Journal of Hydroelectric Engineering* **34** (10), 42–50.

Zheng, Z. F., Gao, H. & Wang, Z. W. 2014 Analysis on spatial distribution of precipitation in Beijing and its city effect. *Plateau Meteor* **33** (02), 522–529.

First received 11 October 2020; accepted in revised form 2 December 2020. Available online 14 December 2020